CLM-P198

United Kingdom Atomic Energy Authority

RESEARCH GROUP

Preprint

TEMPERATURE AND DENSITY MEASUREMENTS IN THE MIDPLANE OF A LONG THETA PINCH

A. D. BEACH
H. A. B. BODIN
C. A. BUNTING
D. J. DANCY
G. C. H. HEYWOOD
M. R. KENWOOD
J. McCARTAN
A. A. NEWTON
I. K. PASCO
R. PEACOCK
J. L. WATSON

Culham Laboratory
Abingdon Berkshire

1969

UNCLASSIFIED
Approved for Publication

CLM-P 198

TEMPERATURE AND DENSITY MEASUREMENTS IN THE MIDPLANE OF A LONG THETA PINCH

by

A.D. BEACH, H.A.B. BODIN,
C.A. BUNTING, D.J. DANCY,
G.C.H. HEYWOOD, M.R. KENWOOD,
J. McCARTAN, A.A. NEWTON,
I.K. PASCO, R. PEACOCK,
J.L. WATSON

A B S T R A C T

This paper describes the measurement of the plasma parameters in an 8 metre long theta pinch. The plasma in the midplane is found to be free of end effects and energy loss for some tens of microseconds and is characterised by electron densities of 2-5 $\times 10^{16}$ electrons/cc and temperatures of 100-300 eV. The measured radial distributions of temperature and density and their dependence on voltage and filling pressure were in agreement with M.H.D. code calculations using an anomalous resistivity previously shown to account for the diffusion in the early stages.

UKAEA Research Group,
Culham Laboratory,
Abingdon,
Berks.

March, 1969.

C O N T E N T S

1. INTRODUCTION

A theta pinch with a coil 8 metres long was built to produce a deuterium plasma, free of end effects for some tens of microseconds, with temperatures in the range 100–300 eV and densities between $2 \sim 5 \times 10^{16}$ electrons/cc. The MHD stability and diffusion of this plasma have been described elsewhere[1–4]; this paper presents and analyses the detailed density and temperature measurements.

The heating and energy loss in a low density theta pinch with zero initial bias field have been discussed by a number of authors[5–8], and in nearly all cases end effects such as thermal conduction[9] and particle flow[8] have an important influence after a few microseconds. In contrast, in the experiment reported here, measurements confirm theoretical predictions that axial processes can be neglected in the midplane for 20–40 μsec, depending on conditions. Thus results during this time can be compared with a radial one-dimensional MHD code[10]. The interpretation of the results is further simplified because the plasma is collision dominated and the ion and electron temperatures are expected to be equal during most of the discharge. In addition, the effects due to radiation cooling from added impurities can be more readily identified in the absence of competing axial loss mechanisms.

Comparing the present experiment with other high power theta pinches, using shorter coils[5–8], the peak magnetic field of 25 kG is considerably smaller, as is the rate of rise of field and consequently the ion temperature. However, in experiments with shorter coils the electron temperature is usually limited by thermal conduction to about 300 eV, a value comparable with that obtained in the present work.

The radial electron temperature distribution in the midplane of the coil was determined by Thomson scattering. The relative electron density distribution was determined by three independent methods - laser light scattering and by spatially resolving the visible continuum emission, using a calibrated image converter camera and a 10-channel fibre bundle assembly[11]. The results for these three methods will be compared. The absolute density was obtained from the mass oscillations[12]. An analysis of the plasma diamagnetism in conjunction with the density distribution gave an independent value of the transverse pressure and beta.

The results are compared with a computation based on a modified MHD code which includes an anomalous resistivity due to micro-instabilities driven by electron-ion streaming. It was shown previously[14] that this resistivity could account for the

enhanced diffusion found in the early stages; thereafter the micro-instability is predicted to be quenched and the resistivity reverts to the Spitzer value, in agreement with the observed classical diffusion[15]. In this paper the radial and temporal variations of temperature and density and their dependence on filling pressure and bank voltage were all found to be in satisfactory agreement with the computations.

2. EXPERIMENTAL DETAILS

The parameters of the 8 metre experiment are similar to those already reported[2]. The coil length was 771 cm and its internal diameter 11 cm. The bore of the clear quartz tube was 8.3 cm. The measurements were carried out at initial deuterium pressures of 10 and 20 mtorr and for bank voltages of 30, 34 and 40 kV which correspond to peak magnetic fields of 19, 21.5 and 25 kG respectively. The peak field was reached in 5.5 μsec and decayed with a time constant of 180 μsec when crowbarred using 32 solid dielectric switches. The gas was preionized by means of an axial current pulse of approximately 10 kA lasting for 8 μsec starting some 15 μsec before the main field was applied. The degree of ionization was estimated by a subsidiary experiment[16] to be above 50%. The characteristics of the main discharge were insensitive to the preionization current, and the impurity content in the preionized plasma was less than 0.1% of oxygen.

3. METHODS OF MEASUREMENT

3.1 Thomson Scattering

A ruby laser developing up to 10^9 W of vertically polarised light in a 20 nsec giant pulse with a beam divergence of 0.7 mrad was mounted at one end of the theta pinch. The beam was focused to a spot 4 mm diameter in the midplane of the coil. The Doppler broadened scattered light emerging horizontally at 90^o to the plasma axis was detected by means of a grating spectrometer[17]. The size of the spectrometer slit and laser spot defined a scattering volume of 0.02 cm^{-3}, giving a vertical resolution of 0.5 mm. The Doppler profile was obtained from the amplitudes at 12 wavelengths measured by 12 synchronously gated photomultipliers, which monitor one half of the profile from 6943 Å downwards, with a resolution of 25 Å. The last channel contained little or no scattered signal but allowed useful recording of the bremsstrahlung emitted along a chord of the plasma which can lead to an independent value of the density distribution[18]. The signals from these multipliers were successively delayed by 75 nsec and displayed serially on a fast oscilloscope. The envelope of the pulse peaks in the resulting oscillogram (Fig.1) gives the scattered light

spectrum directly. The electron temperature was computed by making a least squares fit to a Gaussian curve for the 12 wavelength points. The radial temperature distribution was obtained from a series of discharges by scanning the laser beam and spectrometer field of view across the vertical diameter of the plasma. The relative density distribution was obtained by comparing the total power scattered at each position. This method does not yield reliable data in the outer regions of the plasma. The laser power was monitored with a fast vacuum photodiode.

The system was calibrated to an accuracy of 5-10% using the bremsstrahlung from the plasma as a standard light source varying spectrally as λ^{-2}. The curve fitting accuracy varied from 5 - 20%, but most of the data could be fitted to between 5 and 10%. The electron temperature was thus accurate to ± 15% whilst the accuracy of the distribution depended on the reproducibility of the discharge.

3.2 Density Distribution Measurements from the Visible Continuum

Light from the visible continuum was measured by viewing the plasma radially along a number of parallel chords, from which the density distribution is then obtained using an Abel inversion. In the fibre bundle technique[11], a line-free region of the spectrum is selected by means of an intereference filter 10 Å wide at a wavelength of 4978 Å. The spatial resolution is obtained by means of a 10-channel fibre bundle assembly feeding 10 photomultipliers. This method is not affected by line radiation from the plasma nor from stray scattered light other than in the narrow wave band of the filter. The calibrated camera gives much better spatial resolution (equivalent to 40 channels) but integrates over the whole visible spectrum determined by the S11 photocathode (3000-6500 Å); this method can be affected by line radiation and when obtaining distributions it is assumed that the impurity ions (if any) are homogeneously distributed in the plasma. The camera is calibrated immediately before each discharge with a step wedge having 20 steps, illuminated by a tungsten flash light; the image of the wedge is positioned on the film alongside the area where the plasma light will be recorded. Microdensitometry of the film and calibration is carried out and the data fed into a computer which calculates the density distribution. A correction was applied for background light which was reduced to about 2% of the peak intensity by sand-blasting the tube opposite the viewing slit and backing it with black paper.

The absolute value of electron density was obtained by equating the line density computed from the continuum measurements to the filling line density, which agreed within 20% with the plasma mass, obtained from the mass oscillations[12]. For relative measurements

the accuracy of calibrated camera technique is about 10% near the axis. Stereoscopic streak photographs confirmed that the plasma was cylindrically symmetric during the measurements.

Fig.2 shows density distributions obtained by the three techniques described above; since the data from both the continuum methods was normalised to the filling line density the comparison between them is, in effect, an absolute one. The relative distribution obtained from Thomson scattering was normalised to the other two near the axis. There is more scatter on points obtained from the laser measurement because the distribution has to be built up over a number of discharges, whereas the whole profile is obtained on one discharge with the other methods. The points from the three methods agree within the experimental error. This agreement in the shape of the distribution between the laser method and the continuum methods was particularly satisfactory because of the different physical assumptions involved in the measurements. The agreement between the calibrated camera technique and the others justified the assumptions involved in using radiation from a large region of the visible spectrum. Most of the measurements of the density distribution were made using this method.

3.3 Diamagnetic Loop

The measurements of the plasma diamagnetism[19], analysed in conjunction with the density distribution, allows an independent estimate of average temperature and beta. Assuming a uniform temperature distribution the integral equation for the diamagnetic signal is

$$S = 2\pi B_e \int_0^{r_{wall}} \left[1 - \sqrt{1 - \beta(0)\ n(r)/n(0)} \right] r\ dr$$

where B_e is the external magnetic field. This equation is solved with the measured $n_e(r)$ to find $\beta(0)$, the value of β on axis. The method does not depend on the absolute value of either $(T_e + T_i)$ or $n(0)$, the value of n on the axis. If two of these three quantities are known then the other may be inferred. In practice this method is used to show that $T_i = T_e$.

4. EXPERIMENTAL RESULTS

The temperature and density were measured in the midplane of the coil, and, unless otherwise stated the values on the axis and at peak magnetic field are given. For comparison the values computed from the Hain-Roberts MHD code modified to incorporate a non-classical resistivity (see Section 5) are shown.

4.1 Electron Temperature

Fig.3 shows the measured electron temperature on the axis as a function of the filling pressure at voltages of 34 and 40 kV. It is seen that the temperature rises to about 400 eV at 5 mtorr and 40 kV; the increase in temperature as the pressure is reduced is slightly more marked at 40 kV. Fig.4 (upper portion) shows the electron temperature as a function of radius at 40 kV; the measured temperature is approximately constant over the greater part of the plasma, in agreement with theory, but falls off in the outer regions where the density (Fig.4, lower portion) decreases, in contrast to the theoretical curve, which rises towards the edge (see Section 5). The lower graph (Fig.4) shows the density distribution obtained from Thomson scattering, normalised to the theoretical curve on the axis. Fig.5 shows the electron temperature as a function of time, together with theoretical curves. Up to peak field the theory was computed from the modified MHD code, and thereafter calculated from adiabatic theory assuming a uniform radial distribution of plasma and magnetic field. The dashed theoretical curves from peak field onwards included radiation cooling, introduced at that time, for 10% added oxygen impurity, assuming a coronal model.

The observed time variation of electron temperature with and without added oxygen impurity is shown in Fig.6 - the effect of 2% oxygen is first seen at about 2 μsec and the peak temperature is reduced from about 220 eV to 140 eV. The percentage of oxygen impurity was estimated by measuring the intensity of an OII doublet centred at 4593 Å as a function of the fraction of oxygen impurity added to the initial gas filling; the results are shown in Fig.7.

4.2 Electron Density

Fig.8 shows that the electron density on the axis increases approximately linearly with filling pressure. The light scattering data is normalised to theory at 20 mtorr. Fig.9 shows the measured time variation of the electron density on the axis for a crowbarred discharge determined from both the calibrated camera and light scattering techniques. The data agrees closely with theory. In Fig.10 time development of the density distribution is shown; the theoretical curves assume classical diffusion and no energy loss. In Fig.11 the line density is plotted as a function of time for crowbarred discharges at 34 and 40 kV and 20 mtorr; in both cases the line density was constant for the duration of the measurement, which was limited because the plasma lost its cylindrical symmetry due to the end-induced instability (Section 4.4).

4.3 Plasma Diamagnetism and β

Fig.12 shows the measured diamagnetic signal as a function of time and the theoretical curve calculated assuming the simple model of a uniform mixture of plasma and magnetic field and no energy loss. There is no evidence of the rapid energy loss observed in shorter coil experiments[9], and except for a small discrepancy between 10 and 15 μsec, experiment and theory are in good agreement until 20 μsec - thereafter the experimental points fall rapidly.

The value of β on the axis was calculated from the temperature and density assuming equal ion and electron temperatures, an assumption justified by the short ion-electron energy equipartition time of the order of 1 μsec. This value of beta ($\beta = .8 \pm .2$ at 34 kV, 20 mtorr D_2) agreed with that calculated from the diamagnetic signal within the experimental error.

4.4 Stability

The stereoscopic streak photographs taken at the midplane (Fig.13) show that the plasma is stable and lies close to the tube axis for some 25-30 μsec at 34 kV and 20 mtorr. There is a small lateral motion less than the radius during this time. Thereafter a hydromagnetic instability - a mixture of $m = 1$ and $m = 2$ - appears, which is belived to be due to end effects since its onset time is directly proportional to the tube length[14] and is approximately given by the Alfvén transit time from the ends to the midplane.

5. DISCUSSION

5.1 Particle and Energy Losses

In order to estimate the particle losses numerical computations were carried out using a two-dimensional ideal MHD code in r and z which was developed at Garching[20]; the measured plasma properties at peak magnetic field were used as the initial conditions. These calculations showed no particle losses in the midplane for some 40 μsec for a discharge at 120 eV. This is in agreement with estimates based on the work of Wesson[21], which shows that a rarefaction wave should travel towards the midplane with a velocity $V = C_s \sqrt{1-\beta}$. The experimentally observed constant line density for at least 25 μsec at 120 eV and at least 20 μsec at 160 eV (Fig.11) is consistent with these estimates. The plasma confinement was limited by the end-induced instability and not particle flow from the ends.

Energy losses were studied by measuring the electron temperature as a function of time and from the plasma diamagnetism. Both these methods indicated an absence of energy

loss for at least 20 μsec for the discharge at 34 kV and 20 mtorr (T_e = 120 eV). The diamagnetic signal (Fig.12) reveals an energy loss at about 25 μsec which is correlated with the onset of the end-induced MHD instability. The density distribution expands at this time in the manner expected if there are radial particle losses. The experimental value of the cooling time calculated from these measurements is more than 100 μsec for the discharge at 120 eV.

The value of the thermal conduction cooling time can be calculated from

$$\tau_c = \frac{L}{v_e} \cdot \frac{L}{\lambda_{ee}}$$

where L is the tube half-length, v_e the electron thermal velocity and λ_{ee} the electron mean free path. This time is sensitive to the electron temperature and the values obtained ranged from 100 μsec for the discharge at 10 mtorr and 40 kV (T_e = 240 eV) to about 400 μsec for a discharge at 34 kV and 20 mtorr (T_e = 120 eV). Since there may be some correction required to the thermal conduction coefficient the results may be more usefully compared with the scaling law for the 'limiting temperature'[9], i.e.

$$T_{e(max)}^{7/2} \propto \omega B^2 L^2.$$

Using past data[2], it is predicted that $T_{e(max)} \approx$ 400–450 eV for this experiment.

The data in Fig.5 shows that impurity cooling has relatively little effect after peak magnetic field. The calculation is sensitive to the fraction of oxygen VII remaining in the discharge but at these temperatures theoretical estimates indicate that this state should be almost completely burnt through. The impurity concentration was estimated from Fig.7 to be between ½ and ¾% so it is concluded that radiation losses can be neglected in these experiments. It is important to note that this analysis refers to times after peak magnetic field when the temperature is 100 eV or higher and the intense line radiation from lithium-like ions (OVI) is greatly reduced since this species is rapidly burnt through. During the earlier stages, when the plasma is being heated, the temperature is much more sensitive to the presence of impurities. This was seen in Fig.6 in which the addition of 2% of oxygen impurities reduced the peak electron temperature by some 50%. The temperature is first affected by impurities at about 50 eV, which is believed to be due to the radiation of OVI which is expected to be dominant between 20 and 70 eV. Differences arising at these lower temperatures are maintained due to the subsequent compression, even although the radiation cooling becomes small at later times. The relatively large overall reduction in the temperature from 2% of oxygen in the present experiment is in contrast to

experiments with much higher rates of energy input[9] in which some 5% of added impurity had relatively little effect on the peak temperature.

5.2 Comparison between Results and a Modified MHD Code

A comparison between the experimental results and computations based on the ideal MHD code indicated two important discrepancies; firstly, the observed radial density distribution was of Gaussian form rather than the square distribution predicted, and secondly, the measured value of beta on the axis was about 0.8 compared with the theoretical value of unity. It has been shown[2] that these differences can be explained by the presence of an anomalously high plasma resistivity during the early stages of the discharge, which is believed to be due to micro-instabilities excited by electron-ion streaming. In a non-isothermal plasma with $T_e > T_i$ ion acoustic waves are generated[22] while for an isothermal plasma another high frequency wave is possible[23]. These instabilities occur when the electron ion drift velocity V_D exceeds a critical velocity V_c where $V_c \approx V_s$ the sound speed. Expressions for the resistivity due to such processes have been derived by Sagdeev[13] and have been used to replace the classical value in the MHD code when $V_D > V_c$. Good agreement between theory and experiment was found for the shape of the density distribution and β.

The computed results are insensitive to the choice of possible streaming instabilities when their magnitude and scaling are approximately the same. It is found that the anomalous resistivity reverts to the classical value after ≈ 1 μsec when $v_D \lesssim v_s$. This observation, which is in agreement with the data in Figs.9 and 10 given in this paper, and is discussed elsewhere[2,14], shows classical behaviour of the density distribution after the early stages.

The results given in Figs.3, 5 and 6 show that the dependence of the electron temperature on pressure and voltage and its time variation, also agree with theory. In particular, the measured electron temperature increases continuously when the filling pressure is reduced, as predicted, up to about 400 eV at 5 mtorr (Fig.3); this contrasted with experiments in shorter coils[9] where, due to the thermal conduction limitation, the temperature was about 300 eV and hardly dependent on initial pressure below 50-100 mtorr. A continuous increase of electron temperature with bank voltage was also found.

The electron temperature is approximately constant over most of the plasma radius as expected theoretically (Fig.4), although rather below theory in the conditions shown. However, in the outer-regions where the density becomes small the measured temperature

falls and the computed value increases. This effect, found with both the classical and modified codes, arises principally because the joule heating per particle increases continuously as density falls. Only a very small axial heat loss or increased radial transport is required to remove the effect. Estimates suggest that thermal conduction cooling in the outer region is fast enough to explain the observations; because of the low density the heat loss required is negligible compared with the energy content of the whole plasma, for which the thermal conduction cooling time is some hundreds of microseconds (see Section 5.1 above).

At filling pressures above 10 mtorr differences in the electron temperature at peak field between the ideal and modified codes are less than 10%. This is because although there is some additional electron heating in the early stages, it is compensated by reduced irreversible ion heating, due to the trapped field resulting from the diffusion associated with the enhanced electron heating. In addition, there is substantial adiabatic compression heating of both ions and electrons. At lower filling pressures large differences between the two codes are found, which will be discussed elsewhere[24]. The MHD code is expected to give a much better description of the collisional plasma ($T_e \sim T_i$) obtained in the present experiment, than for discharges with very high perpendicular ion energies[25] in which the ion heating and relaxation is not yet fully understood. In theta pinch experiments using much shorter coils[9] agreement with the code could only be obtained by including a large energy loss term in the computations.

6. CONCLUSIONS

A theta pinch experiment has been carried out in which the length of the coil has been increased to 8 metres in order to delay the effects of the ends. The plasma has a density between 2 and 5 $\times$ 10^{16} cm^{-3} and an electron temperature which can be varied between 100 and 400 eV by changing the filling pressure and bank voltage. The plasma is collisional and the ion and electron temperatures are approximately equal during most of the discharge. The measured line density is constant for some 25 μsec for the discharge at 160 eV and is in agreement with predictions based on a two-dimensional MHD code and an analytical model which shows that the midplane should be free of particle losses for 40 μsec in these conditions. An analysis of the diamagnetic signal and the electron temperature as a function of time show that in the midplane the plasma is free of all energy loss within the experimental error of 10 to 20% for about 20 μsec at 120 eV, and 10 μsec at 240 eV. In all conditions studied the plasma lifetime in the midplane is

limited by a hydromagnetic instability, believed to originate at the ends, and not by particle losses (radial diffusion or axial flow) or by energy losses. A value of the cooling time has been estimated from these results to be more than 100 μsec which is comparable with the values calculated for radiation at the measured impurity concentrations of ½ to ¾% and from thermal condution to the ends. The electron temperature and density distributions, their dependence on filling pressure and capacitor bank voltage, and their time variation all agree within the experimental error of 20% with theory. This is based on a modified MHD code, which uses a non-classical resistivity due to micro-instabilities in the early stages, previously shown to account for the diffuse current sheath and value of beta on the axis of less than unity.

7. ACKNOWLEDGEMENTS

The authors wish to thank N.J. Peacock for useful discussions and L. Firth for providing the preionization system.

8. REFERENCES

1. BODIN, H.A.B., NEWTON, A.A., WOLF, G.H. and WESSON, J.A. Culham Laboratory CLM-P 184 (1969).

2. BODIN, H.A.B. and NEWTON, A.A. Culham Laboratory CLM-P 185 (1969). To be published in Phys. Fluids.

3. BODIN, H.A.B. 3rd European Conf. on Controlled Fusion and Plasma Physics, Stockholm (1967).

4. BODIN, H.A.B. Los Alamos Report LA-3770, Paper A-2 (1967).

5. GOLDMAN, L.M., POLLOCK, H.C., REYNOLDS, J.A. and WESTERDORP, W.F. Phys. Rev. Letters 9 (1962) 361.

6. QUINN, W.E., LITTLE, E.M., RIBE, F.L. and SAWYER, G.A. Plasma Physics and Controlled Nuclear Fusion Research (Proc. Conf. Culham, 1965) 1, IAEA, Vienna (1966) 237.

7. ANDELFINGER, C., DECKER, G., FUNFER, E., HEISS, A., KEILHACKER, M., SOMMER, J. and ULRICH, M. Plasma Physics and Controlled Nuclear Fusion Research (Proc. Conf. Culham, 1965) 1, IAEA, Vienna (1966) 249.

8. BODIN, H.A.B., GREEN, T.S., NEWTON, A.A., NIBLETT, G.B.F. and REYNOLDS, J.A. Plasma Physics and Controlled Nuclear Fusion Research (Proc. Conf. Culham, 1965) 1, IAEA, Vienna (1966) 193.

9. GREEN, T.S., FISHER, D.L., GABRIEL, A.H., MORGAN, F.J. and NEWTON, A.A. Phys. Fluids 10 (1967) 1663.

10. HAIN, G., HAIN, K., KOPPENDORFER, W., ROBERTS K.V., and ROBERTS S. Z. Naturf. 15a (1960) 1039.

11. DANCY, D.J. and KEILHACKER, M. Culham Laboratory CLM-M 55 (1965).

12. BODIN, H.A.B. and McNAMARA, B. Plasma Phys. 9 (1967) 505.

13. SAGDEEV, R.J. Proc. Symp. in Appl. Maths., (1965) American Math. Soc., XVIII, (1967) 281.

14. BODIN, H.A.B., McCARTAN, J., NEWTON, A.A. and WOLF, G.H. 3rd Conf. Plasma Physics, Novosibirsk (1968), Paper CN-24/K-1.

15. SPITZER, L. Physics of Fully Ionized Gases, Interscience (1962).

16. NEWTON, A.A. Culham Laboratory CLM-R 62 (1966).

17. BEACH, A.D. AWRE Report O-42/67 (1967).

18. WATSON, J.L. and BEACH, A.D. Brit. J. Appl. Phys. (J. of Phys. D) 2 (1969) 169.

19. GREEN, T.S. Nucl. Fusion 2 (1962) 92.

20. SCHNEIDER, W. Thesis, Garching (1968).

21. WESSON, J.A. Plasma Physics and Controlled Nuclear Fusion Research (Proc. Conf. Culham, 1965) 1, IAEA, Vienna (1966) 223.

22. STRINGER, T.E. J. Nucl. Energy. Pt.C 6 (1964) 267.

23. HAAS, F. Private communication.

24. BODIN, H.A.B. et al. To be published.

25. FUNFER, E. Los Alamos Report LA-3770, Paper A-1 (1967).

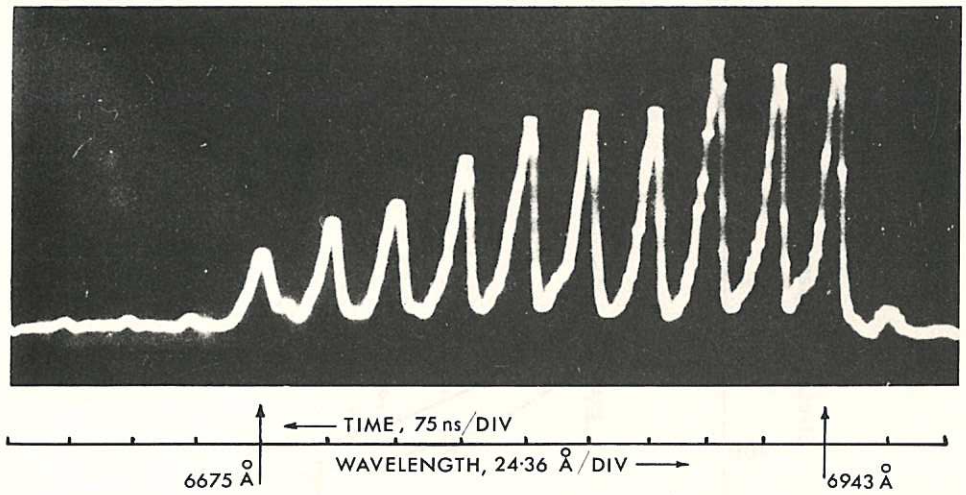

Fig. 1 (CLM-P 198)
Oscillogram from 12 channel spectrophotometer showing a spectrum of scattered laser light

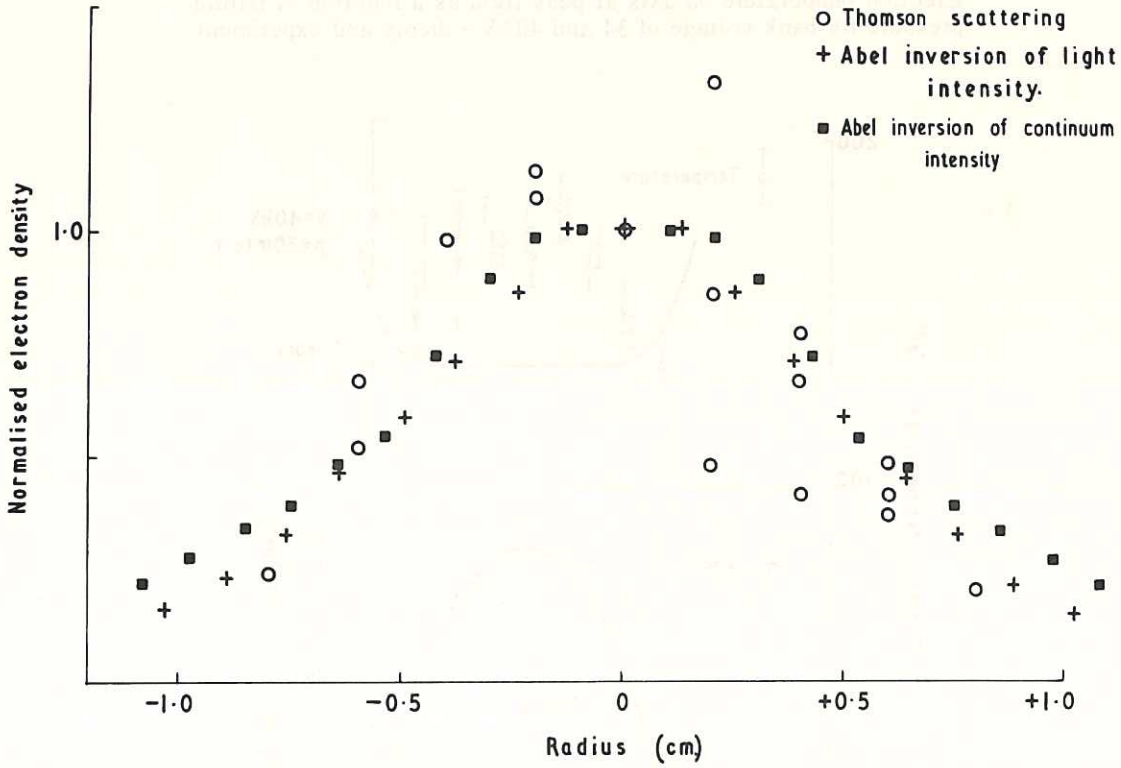

Fig. 2 (CLM-P 198)
Radial electron density distributions obtained by three different techniques

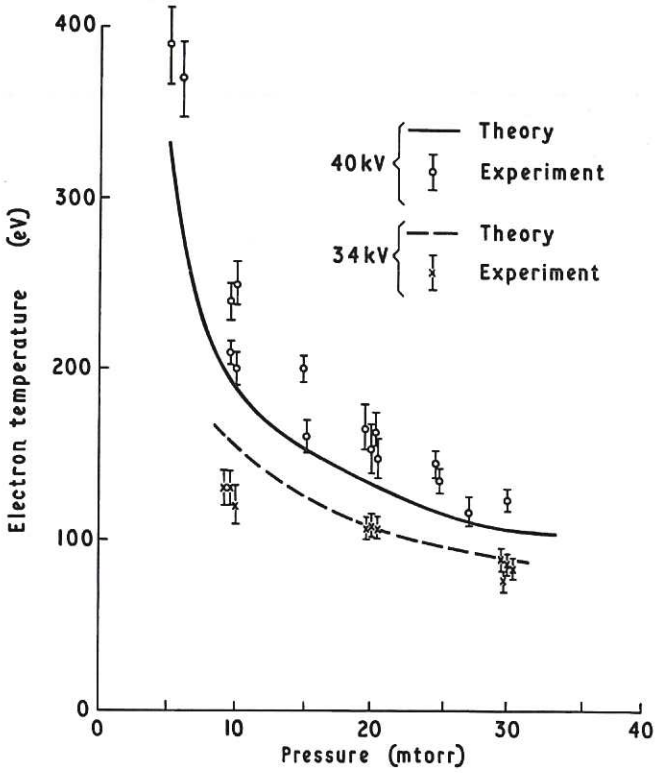

Fig. 3 (CLM-P 198)
Electron temperature on axis at peak field as a function of filling pressure for bank voltage of 34 and 40 kV - theory and experiment

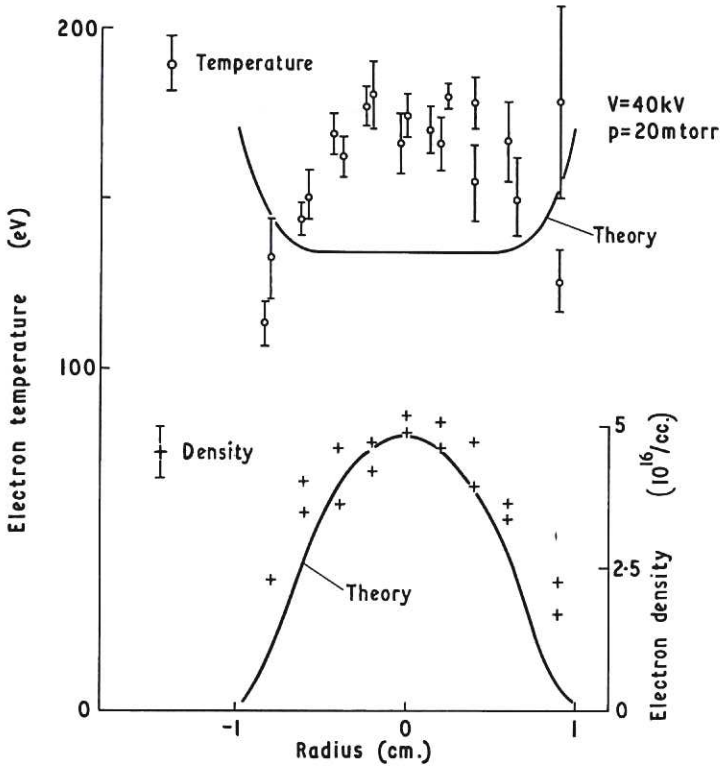

Fig. 4 (CLM-P 198)
Radial distributions of electron temperature (above) and density (below) at peak magnetic field, both obtained from Thomson scattering. Theoretical distributions also shown (40 kV and 20 mtorr)

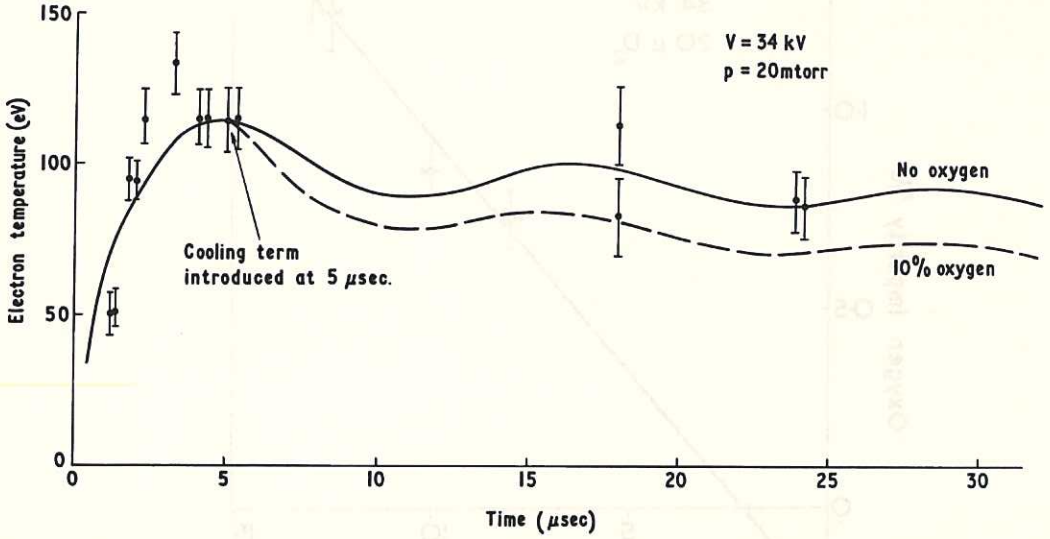

Fig. 5 (CLM-P198)
Time variation of electron temperature on axis — experiment and theory assuming no energy loss (full line) and radiation cooling (dashed line) introduced at 5 μsec, due to 10% oxygen impurity (34 kV, 20 mtorr)

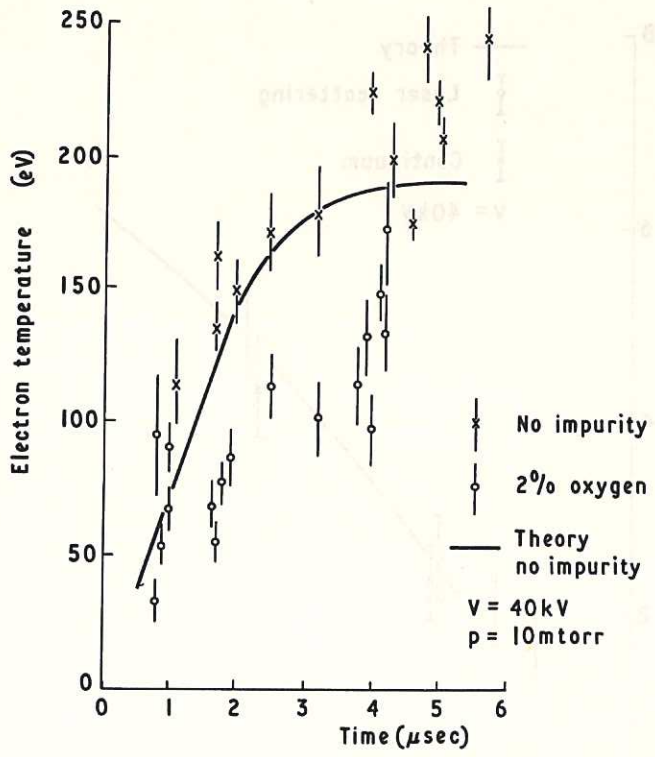

Fig. 6 (CLM-P198)
Measured time variation of electron temperature on axis up to peak field for discharges with zero and 2% added oxygen impurity (40 kV, 10 mtorr). Theoretical variation shown for no added impurity

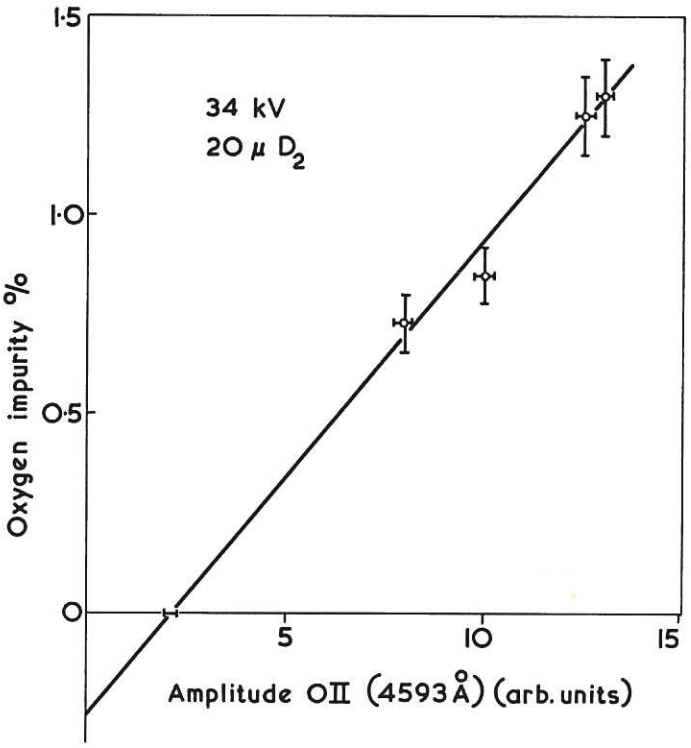

Fig. 7 (CLM-P 198)
Amplitude of oxygen II line (4593 Å) as a function of added oxygen impurity concentration (34 kV, 20 mtorr)

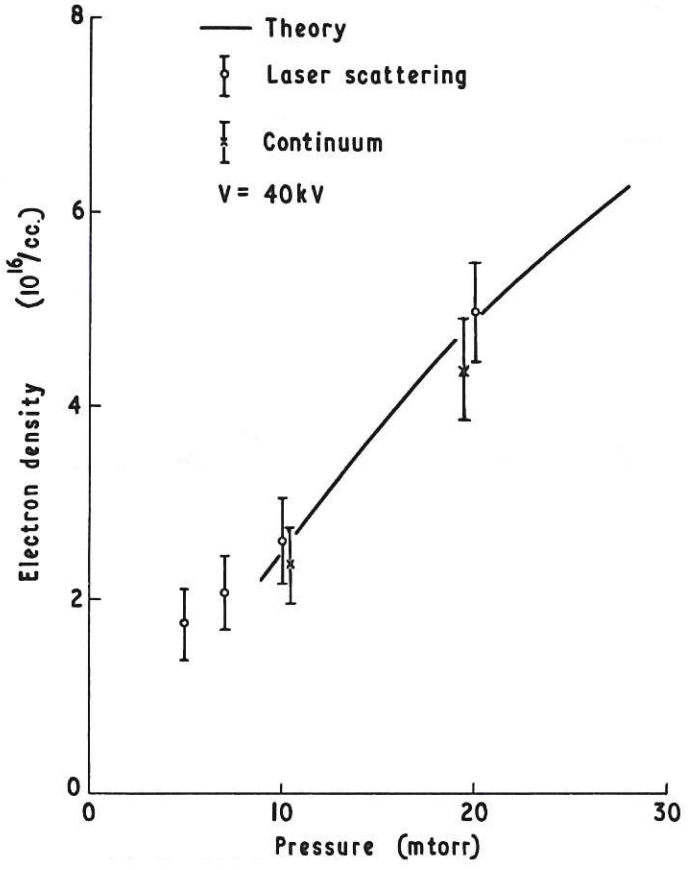

Fig. 8 (CLM-P 198)
Electron density on axis at peak magnetic field as a function of filling pressure - experiment and theory (40 kV)

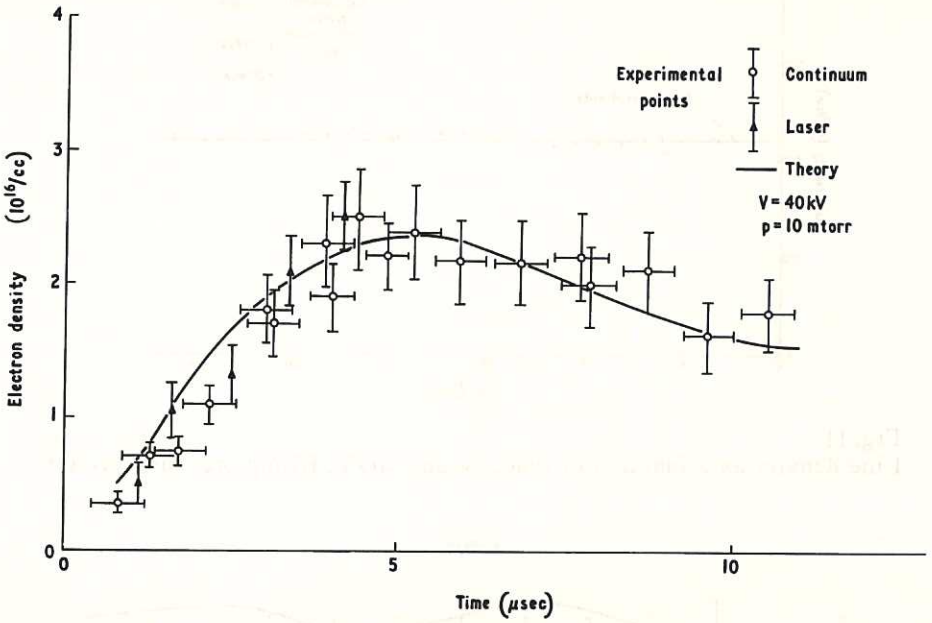

Fig. 9 (CLM-P 198)
Electron density on axis obtained from Thomson scattering and from the visible continuum as a function of time – theoretical curves are also shown (40 kV, 10 mtorr)

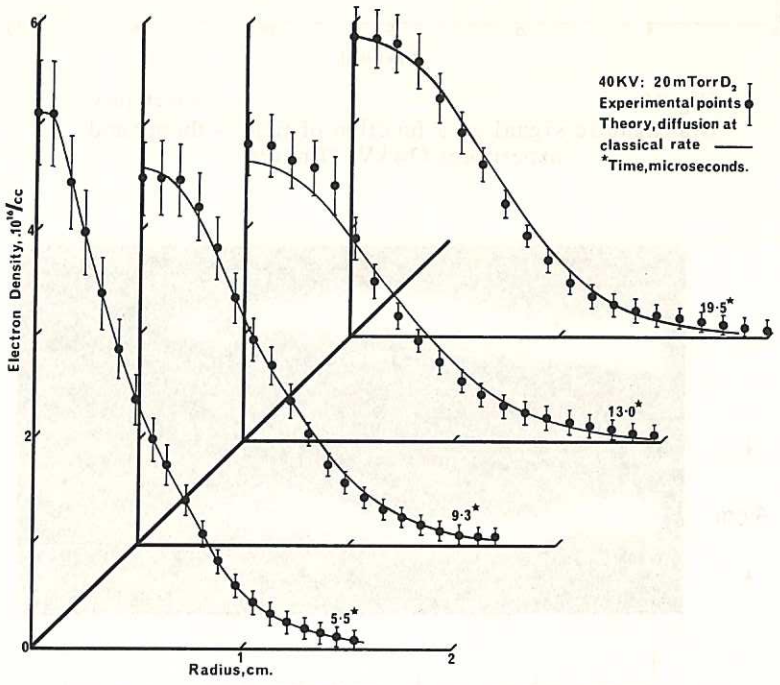

Fig. 10 (CLM-P 198)
Density distribution at four different times – experimental points and theoretical curve assuming classical resistivity (40 kV, 20 mtorr)

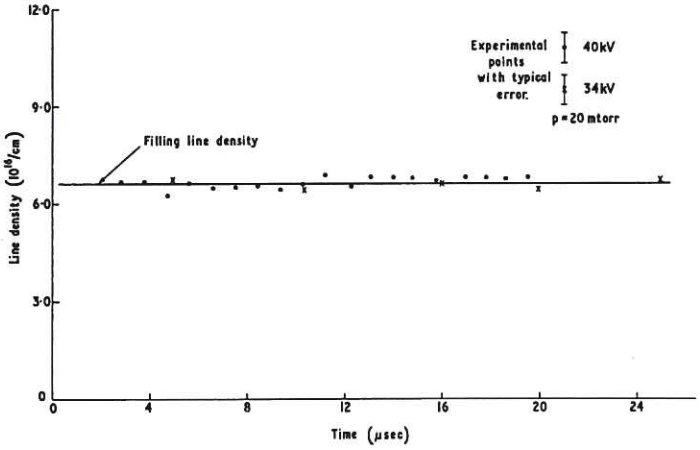

Fig. 11 (CLM-P 198)
Line density as a function of time, 34 and 40 kV; filling pressure 20 mtorr

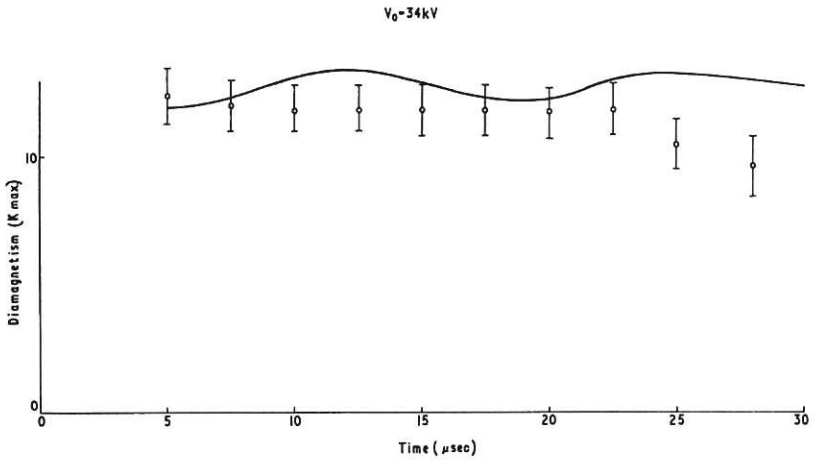

Fig. 12 (CLM-P 198)
Diamagnetic signal as a function of time — theory and experiment (34 kV, 20 mtorr)

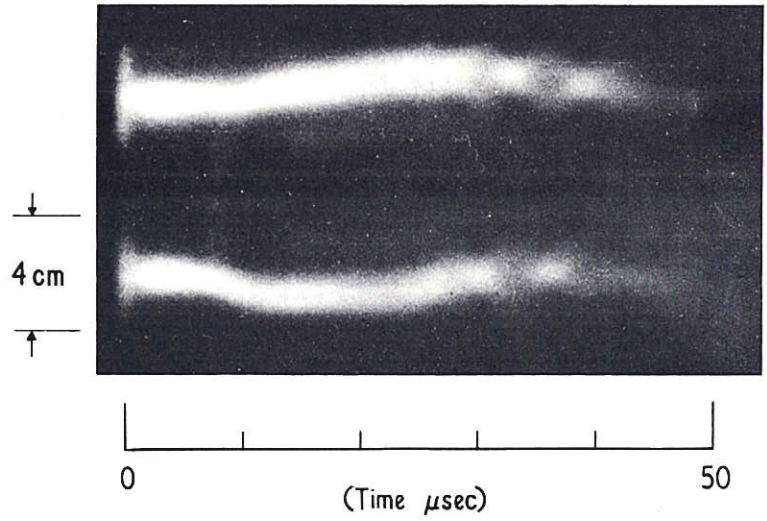

Fig. 13 (CLM-P 198)
Stereoscopic streak photographs taken in the midplane for a discharge at 34 kV, 20 mtorr. Note that only part of the tube cross-section is shown